New insight in the nature of surface magnetic anisotropy in iron borate

M. Strugatsky, K. Seleznyova, V. Zubov, J. Kliava

New insight in the nature of surface magnetic anisotropy in iron borate

M. Strugatsky [a], K. Seleznyova [a,b], V. Zubov [c], J. Kliava [b,*]

[a] Physics and Technology Institute, V.I. Vernadsky Crimean Federal University, 4 Vernadsky Avenue, 295007 Simferopol, Russia
[b] LOMA, UMR 5798 Université de Bordeaux-CNRS, 33405 Talence cedex, France
[c] Moscow State University, Leninskie Gory, 119991 Moscow, Russia

ARTICLE INFO

Keywords:
Iron borate $FeBO_3$
Surface magnetic anisotropy
Crystal field
Superposition model

ABSTRACT

The theory of surface magnetism of iron borate, $FeBO_3$, has been extended by taking into consideration a crystal field contribution to the surface magnetic anisotropy energy. For this purpose, a model of distortion of the six-fold oxygen environment of iron ions in the near-surface layer of iron borate has been put forward. The spin Hamiltonian parameters for isolated Fe^{3+} ions in the distorted environment of the near-surface layer have been calculated using the Newman's superposition model. The crystal field contribution to the surface magnetic anisotropy energy has been calculated in the framework of the perturbation theory. The model developed allows concluding that the distortions of the iron environment produce a significant crystal field contribution to the surface magnetic anisotropy constant. The results of experimental studies of the surface magnetic anisotropy in iron borate can be described assuming the existence of relative contractions in the near-surface layer of the order of 1 %.

1. Introduction

Iron borate, $FeBO_3$, has rhombohedral calcite type structure with point group symmetry D_{3d} and space group D^6_{3d} [1]. From the stand point of magnetic properties $FeBO_3$ is a two sublattice easy plane anti ferromagnet possessing weak ferromagnetism and the Néel temperature $T_N \approx 348$ K [1]. Within the accuracy of experiments, the sublattice mag netization vectors lie in the basal plane, (0 0 0 1) in hexagonal coordi nate system, and are nearly antiparallel [1]. However, because of a slight departure from anti parallelism, apart from a strong antiferromagnetic moment $\boldsymbol{L} = \mathfrak{M}_1 - \mathfrak{M}_2$, a weak ferromagnetic moment $\boldsymbol{M} = \mathfrak{M}_1 + \mathfrak{M}_2$ occurs, $\mathfrak{M}_1$ and $\mathfrak{M}_2$ being the magnetizations of two sublattices with a norm $\mathfrak{M}$.

Iron borate can be synthesized by two routes: (i) from the solution in the melt and (ii) from the gas phase [2,3]. The gas phase technique allows obtaining bulk single crystals of iron borate with large *non basal* faces of optical quality. The existence of natural non basal faces has al lowed finding out and describing a specific magnetic state of a thin near surface layer surface magnetism [4,5] caused by lowering of symme try in the environment of near surface magnetic ions in comparison with those in the crystal volume. Néel was the first to specify the existence of surface magnetic anisotropy in ferromagnets due to this effect [6]. How ever, the manifestation of this anisotropy in conventional ferromagnets is usually obscured by the demagnetizing field and large volume mag netocrystalline anisotropy. In contrast, in the weakly ferromagnetic iron borate crystal the surface magnetic anisotropy can be observed because the demagnetizing field, proportional to the total volume magnetiza tion, is small and the anisotropy in the basal plane is weak [1]. There fore, magnetic characteristics of a thin (0.01 0.1 μm) near surface layer of iron borate drastically differ from those of the volume. Such effects were studied both experimentally, using the magneto optic Kerr effect, and theoretically [4,5].

The surface magnetic anisotropy energy can be calculated as the dif ference of the magnetic energies of ions in the near surface layer and in the crystal volume. This difference is due to two causes: (i) the oc currence of the crystal surface *per se* (neglecting a modification of the oxygen environment of near surface iron ions) and (ii) structural distor tions arising in the near surface layer.

In $FeBO_3$ the exchange energy in a good approximation is isotropic [1]; therefore, the *density* of the surface magnetic anisotropy energy, σ is expected to include dipole dipole, σ_{dip} and crystal field, σ_{cf} contribu tions. Obviously, the cause (i) intervenes only in the calculation of the dipole dipole contribution whereas the cause (ii) is expected to modify both the dipole dipole contribution as a result of alteration of mutual disposition of iron ions in the near surface layer and the crystal field contribution in as much as the oxygen environment of iron ions in the near surface layer undergoes additional distortions in comparison with the crystal volume.

Previously, a theoretical description of σ has been put forward tak ing into account only the cause (i), i.e. neglecting structural distortions in the near surface layer [4]. In this approximation, σ will include only the dipole dipole contribution, and its maximum value will occur for

* Corresponding author.
E-mail address: janis.kliava@u-bordeaux.fr (J. Kliava).

the $(1\,0\,\bar{1}\,4)$ face [4]. It was assumed that the magnetic moments of iron ions in the near surface layer lie in the basal plane; thus, the polar angle ϑ of the reduced antiferromagnetic moment $\boldsymbol{l} = \frac{1}{2}\boldsymbol{L}/\mathfrak{M}$ equals $\frac{\pi}{2}$ [4]. Indeed, a considerable deviation of $\boldsymbol{l}$ from this plane would result in the emergence of a transition magnetic layer, similar to a domain wall, between the crystal volume and the near surface layer. In this layer the magnetization will be non uniformly distributed, so that the equilibrium orientation of $\boldsymbol{l}$ will gradually turn from that in the volume to that in the near surface layer [4]. As far as the transition layer would possess a very significant energy density; of the order of magnitude of $\sqrt{a_{\text{eff}} A} \approx 1.8 \times 10^{-3}\,\text{J m}^{-2}$, ($a_{\text{eff}} \approx 4.85 \times 10^{5}\,\text{J m}^{-3}$ being an effective uniaxial anisotropy constant in the volume and $A \approx 0.7 \times 10^{-11}\,\text{J m}^{-1}$ being the constant in the expression describing exchange interaction in the transition layer), the emergence of this layer would be energetically unfavorable [4]. Thus, in the near surface layer $\boldsymbol{l}$ will lie in the basal plane or make a small angle with this plane, and the azimuthal angle of $\boldsymbol{l}$ in the dipole dipole approximation will be determined by surface magnetic anisotropy [4]:

$$\sigma_{\text{dip}} = a_{S\text{dip}} \sin^2 \varphi \tag{1}$$

where φ is the azimuthal angle of $\boldsymbol{l}$ with respect to the two fold C_2 axis and $a_{S\text{dip}}$ is the dipole dipole contribution to the surface magnetic anisotropy constant. At room temperature $a_{S\text{dip}} = 1.4 \times 10^{-5}\,\text{J m}^{-2}$ [5]. In equilibrium $\boldsymbol{l}$ is parallel to one of the C_2 axes; therefore, the reduced ferromagnetic vector $\boldsymbol{m} = \frac{1}{2}\boldsymbol{M}/\mathfrak{M}$, $\boldsymbol{m} \perp \boldsymbol{l}$, is perpendicular to this axis, so that C_2 is the hard magnetization axis in the basal plane. This result has been confirmed by experimental observations for $(1\,0\,\bar{1}\,4)$ face of the crystal [4].

Applying a magnetizing field $\boldsymbol{H}$ in the basal plane, where the magnetic anisotropy is small, the direction of $\boldsymbol{l}$ in the transition layer will gradually change from that in the volume, determined by $\boldsymbol{H}$, to that in the near surface layer, determined by both $\boldsymbol{H}$ and the surface magnetic anisotropy. The saturation field along the hard magnetization axis in the near surface layer, called the critical field H_c, is considered as the measure of the surface magnetic anisotropy [4]:

$$H_c = \frac{4 a_{S\text{dip}}{}^2}{AM}. \tag{2}$$

where M is the spontaneous magnetization of the crystal. For $FeBO_3$ at room temperature $M = 11.79\text{G}$ [4]. In fact, an application of such a field would totally erase the transition layer.

Zubov et al. have found that on the $(1\,0\,\bar{1}\,4)$ face of iron borate $H_c \approx 1\text{kOe}$ at 300 K; meanwhile, the H_c value calculated with Eq. (2) is much lower, $H_c = 0.2$ kOe [5]. From the preceding analysis we can expect that this discrepancy could be removed if we allow for structural distortions in the near surface layer, ("surface reconstruction"). Earlier, an attempt in this direction has been made; however, only changes in the positions of iron ions have been considered [5]. (In such an approximation, only the dipole dipole contribution to the surface magnetic anisotropy is accounted for.) In this case, the experimental H_c value could be obtained only for relative extensions as large as $7-12\,\%$ [5].

Meanwhile, it is evident that in the near surface layer, the oxygen environment of iron ions undergoes additional distortions in comparison with the crystal volume, giving rise to the crystal field contribution to the surface magnetic anisotropy energy. The aim of the present work is to consider these distortions and to provide a complete description of the surface magnetic anisotropy of iron borate, including both the dipole dipole and crystal field contributions.

2. Surface reconstruction

In the crystal volume, each iron ion is surrounded by six oxygens forming a nearly perfect octahedron. In turn, borons are located at the centers of equilateral oxygen triangles, so that Fe^{3+} cations turn out to be sixfold coordinated by flat $BO_3{}^{3-}$ groups playing the role of anions. EPR studies have revealed the existence of two non equivalent iron sites with local axes rotated through an angle $\pm\alpha$ about the C_3 axis, see Fig. 1 [7].

The smallest rhombohedron with faces of the type $(1\,0\,\bar{1}\,4)$, containing iron ions in all vertices and face centers (face centered cell), is shown in Fig. 2; the faces parallel to the crystal surface are colored. These faces are perpendicular to yz planes. We assume that the distortions of interatomic distances in the near surface layer occur in yz planes.

In the near surface layer, oxygen octahedrons of two non equivalent sites of Fe^{3+} are distorted. Consider the locations of irons and surrounding oxygens for these two sites with respect to the crystal surface. Fig. 3(a) shows the rhombohedron of Fig. 2 turned so that the yz plane is parallel to the plane of the figure, while the crystal surface and the basal plane xy are orthogonal to yz plane. (For simplicity, we show only two non equivalent sites, Fe_1 and Fe_2 and their oxygen environments in the absence of distortions.)

We assume that the distortions in the near surface layer occur only in the oxygen octahedrons nearest to the crystal surface denoted by F in Fig. 3 and passing through $O_1{}^6$ and $O_2{}^6$ oxygens (the subscripts numbering the iron sites and the superscripts numbering the oxygens linked to a given iron site). We can divide the near surface layer into four parallel sub layers separated by planes passing through oxygen and iron ions, see Fig. 3. We assume that the B plane remains immobile, the distortions occur along the AD edge of the rhombohedron, and the displacements of ions lying at different distances from B are proportional to these distances. Fig. 3(b) illustrates this model; for clarity the relative displacements have been exaggerated.

3. Crystal field surface anisotropy

Previously, we have carried out EPR studies of Fe^{3+} in $GaBO_3$ single crystals and determined the spin Hamiltonian parameters using crystallographic data and the Newman's superposition model [7,8].

In order to calculate the crystal field contribution to the surface magnetic anisotropy energy, we have considered the generalized spin Hamiltonian expressed by means of tesseral spherical tensor operators $\mathscr{T}^{l_B l_S}_{lm}(\boldsymbol{n}, \boldsymbol{S})$ where $\boldsymbol{n}$ is the unit vector in the direction of the magnetizing field $\boldsymbol{H}$ and l_B and l_S are powers of $\boldsymbol{H}$ and of the spin operators, respectively [9].

The required form of the spin Hamiltonian can be adapted from Eq. (4) in the paper by Tennant et al. [10], as follows (cf. the review paper by Kliava and Berger [11]):

$$\mathfrak{H} = \sum_{l=2,4} \sum_{m=-l}^{l} \mathscr{B}^{0l}_{lm} \mathscr{T}_{lm}(\boldsymbol{S}) + g_e \beta H \sum_{l_S=1,3,5} \sum_{l=\begin{cases} l_S - 1 \\ l_S + 1 \end{cases}} \sum_{m=-l}^{l} \mathscr{B}^{1l_S}_{lm} \mathscr{T}^{1l_S}_{lm}(\boldsymbol{n}, \boldsymbol{S}). \tag{3}$$

Here the first and second terms on the right hand side are, respectively, zero field ($l_B = 0$) and *linear* Zeeman ($l_B = 1$) spin Hamiltonians; $l = |l_S - l_B|, \ldots, l_S + l_B$ must be even to preserve time inversion invariance. In particular, for $l_B = 0$, $l = l_S$, and for $l_B = 1$, $l = l_S \pm 1$. The $\mathscr{B}^{0l}_{lm}$ parameters in Eq. (3) are proportional to the corresponding Stevens parameters B^m_l, and the procedure of calculating $\mathscr{B}^{1l_S}_{lm}$ is described in detail by McGavin et al. [9].

As far as $\mathscr{B}^{l_B l_S}_{lm}$ are components of rank l irreducible tensors [9,10], they can be consistently expressed within the superposition model, as follows [7,11]:

$$\mathscr{B}^{l_B l_S}_{lm} = \sum_{j=1}^{n} b^{l_B l_S}_{lm}(r_j)\, C^m_l(\vartheta_j, \varphi_j) \tag{4}$$

where j enumerates the nearest neighbors of the paramagnetic ion with spherical coordinates r_j, ϑ_j, ϕ_j, and $b^{l_B l_S}_{lm}(r_j)$ and $C^m_l(\vartheta_j, \varphi_j)$ are, respectively, radial functions and *tesseral* coordination factors; the latter are given in Appendix of the paper by Seleznyova et al. [7].

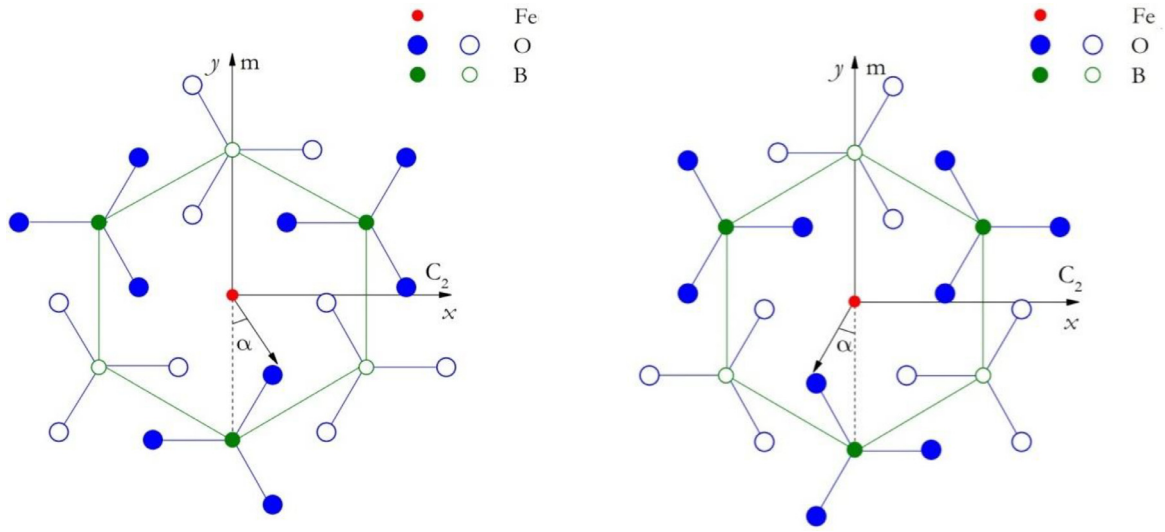

Fig. 1. Two non-equivalent sites of Fe^{3+} in iron borate. The Cartesian coordinate axes are directed as follows: $x \parallel C_2$,y lies in the symmetry plane m and $z \parallel C_3$, the three-fold axis [1]. The z-axis is perpendicular to the plane of the figure and points toward the reader. Full and empty circles represent ions located above and below this plane, respectively.

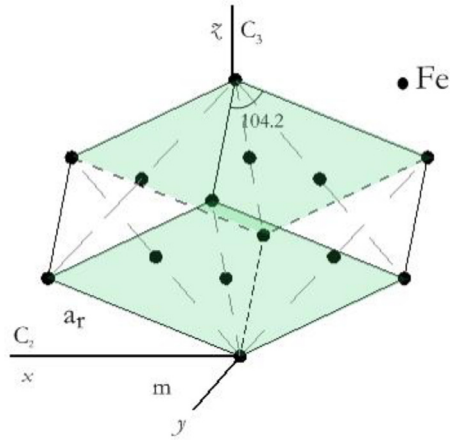

Fig. 2. A rhombohedron with edge length $a_r = 5.862$Å and apex angle 104.2° used to calculate the density of surface magnetic anisotropy energy. The Cartesian coordinate axes are directed as in Fig. 1.

For simplicity, the radial functions have been chosen in the following form:

$$b_{lm}^{l_B l_S}(r_j) = \bar{b}_{l_S}(r_0/r_j)^{t_{l_S}} \tag{5}$$

where $\bar{b}_{l_S}$ are intrinsic parameters, t_{l_S} are the corresponding power exponents and $r_0 = 2.101$ Å is the reference distance corresponding to the average Fe–O distance in MgO [12]. For near surface iron ions, the superposition model parameters are expected to remain the same as for those in the volume, at least as far as distortions in their environment remain weak. We have used the following values of $\bar{b}_{l_S}$ and t_{l_S} [7]:

$$\begin{gathered}\bar{b}_2 = 0.4\text{cm}^{-1}, t_2 = 8\\ \text{and}\\ \bar{b}_4 = 3.1\cdot 10^{-5}\text{cm}^{-1}, t_4 = 5.\end{gathered} \tag{6}$$

The $\bar{b}_3$ and $\bar{b}_5$ parameters turn out to be very small [7], therefore, the corresponding terms in the spin Hamiltonian have been neglected.

On the other hand, the spin Hamiltonian for iron ions in the near surface layer should include terms describing the concomitant lowering of symmetry. Besides, as far as Fe^{3+} ions in the near surface layer of $FeBO_3$ are subject to a strong exchange field, we can use the mean field approximation and substitute an effective exchange field $\boldsymbol{H}_k$ for the magnetizing field $\boldsymbol{H}$ ($k = 1, 2$ numbering the non equivalent iron sites). For the type of distortions described above, the spin Hamiltonian takes the form:

$$\begin{aligned}\mathfrak{H}_k &= g\beta \boldsymbol{H}_k\cdot\boldsymbol{S}_k \pm B_2^{-2}O_{2k}^{-2} + B_2^{-1}O_{2k}^{-1} + B_2^0 O_{2k}^0 \pm B_2^1 O_{2k}^1\\ &\quad + B_2^2 O_{2k}^2 + B_4^0 O_{4k}^0 \pm B_4^3 O_{4k}^3 + B_4^{-3} O_{4k}^{-3}\end{aligned} \tag{7}$$

where g is close to the free electron g factor $g_e = 2.0023$, β is the Bohr magneton, $\mathbf{S}_k$ is the electron spin for the kth Fe^{3+} ion ($S_k = 5/2$); O_{2k}^0, $O_{2k}^{\pm 1}$, $O_{2k}^{\pm 2}$, O_{4k}^0 and $O_{4k}^{\pm 3}$ are the extended Stevens operators [13]; B_{2k}^0, $B_{2k}^{\pm 1}$, $B_{2k}^{\pm 2}$ and B_{4k}^0, $B_{4k}^{\pm 3}$ are, respectively, the second and fourth order fine structure parameters. In Eq. (7) as well as in the subsequent equations the ± signs before certain terms correspond to $k = 1, 2$, respectively.

Assuming the "Zeeman" term $\mathfrak{H}_0 = g\beta \boldsymbol{H}_k\cdot\boldsymbol{S}_k$ in Eq. (7) to be much larger than the remaining terms, we have calculated the energies of the spin levels E_{mk} using the perturbation theory. With this aim in view, we have followed the approach of "correct" zero order wave functions described by Landau and Lifshitz [14]. In the first order of perturbations, we get:

$$\begin{aligned}E_{mk} &= g\beta m H_k + \left[3m^2 - S(S+1)\right]h_{2k}^1\\ &\quad + \left[35m^4 - 30m^2 S(S+1) + 25m^2 - 6S(S+1) + 3S^2(S+1)^2\right]h_{4k}^1\end{aligned} \tag{8}$$

where $S = S_k = \frac{5}{2}$, $m = -\frac{5}{2}, -\frac{3}{2}, \ldots, \frac{5}{2}$ and

$$\begin{aligned}h_{2k}^1 &= \pm\tfrac{1}{2}B_2^{-2}\sin^2\vartheta_k \sin 2\varphi_k + \tfrac{1}{4}B_2^{-1}\sin 2\vartheta_k \sin\varphi_k + \tfrac{1}{2}B_2^0\left(3\cos^2\vartheta_k - 1\right)\\ &\quad \pm\tfrac{1}{4}B_2^1 \sin 2\vartheta_k \cos\varphi_k + \tfrac{1}{2}B_2^2\sin^2\vartheta_k\cos 2\varphi_k;\\ h_{4k}^1 &= \tfrac{1}{8}B_4^{-3}\cos\vartheta_k\sin^3\vartheta_k \sin 3\varphi_k + \tfrac{1}{8}B_4^0\left(35\cos^4\vartheta_k - 30\cos^2\vartheta_k + 3\right)\\ &\quad \pm\tfrac{1}{8}B_4^3\cos\vartheta_k\sin^3\vartheta_k\cos 3\varphi_k.\end{aligned} \tag{9}$$

In the strong exchange case, the spins of two non equivalent iron ions are antiparallel: $\vartheta_1 = \vartheta$, $\varphi_1 = \varphi$, $\vartheta_2 = \pi - \vartheta$, and $\varphi_2 = \varphi + \pi$.

At $T = 0$K, the only occupied spin level is the lowest one (with $m = -\frac{5}{2}$), so that the anisotropic part of the right hand side of Eq. (8) for this level provides the crystal field contribution to the density of the magnetic anisotropy energy of the near surface layer:

$$\sigma_{\text{cf}\,S} = \tfrac{1}{2}N\begin{bmatrix}10B_{2S}^{-1}\sin\vartheta\cos\vartheta\sin\varphi + \left(30B_{2S}^0 - 450B_{4S}^0 + 10B_{2S}^2\right)\cos^2\vartheta + 525B_{4S}^0\cos^4\vartheta\\ +20B_{2S}^2\sin^2\vartheta\cos^2\varphi + 15B_{4S}^{-3}\cos\vartheta\sin^3\vartheta\sin 3\varphi\end{bmatrix} \tag{10}$$

where N is the number of Fe^{3+} ions per unit surface ($N = 6.0036\times 10^{18}\text{m}^{-2}$ for $(10\bar{1}4)$ face) and the S subscript refers to the parameters for the

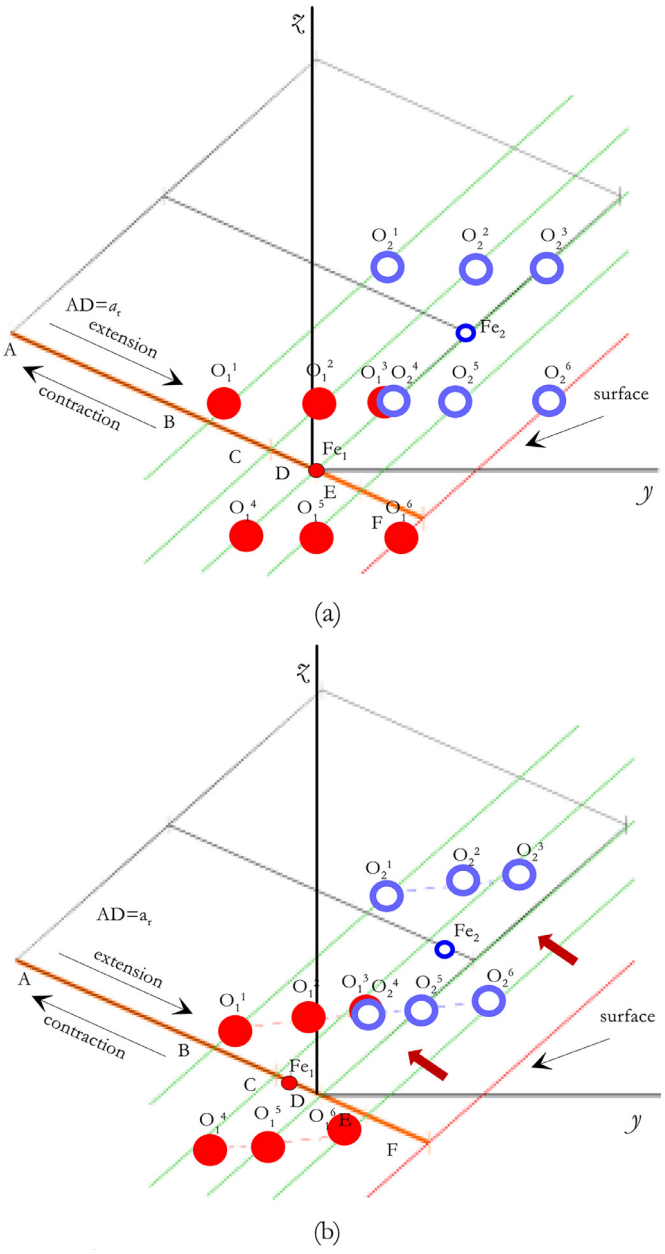

Fig. 3. Two non-equivalent Fe^{3+} sites and their oxygen environments: without distortions (a) and in the case of contraction (b) (full red and empty blue circles for Fe_1 and Fe_2, respectively). The Cartesian coordinate axes are directed as in Fig. 1. The *x*-axis is perpendicular to the plane of the figure and points towards the reader. The nearest-neighboring "top" and "bottom" oxygen triangles for both iron sites have the same *z*-coordinate and different *x*-coordinates. (For interpretation of the references to color in this figure legend, the reader is referred to the web version of this article.)

near surface layer in the presence of distortions. The parameters in Eq. (10) depend on relative distortions, $\varepsilon = \Delta a_r/a_r$ where a_r is the edge length of the rhombohedron shown in Figs. 2 and 3 and Δa_r is the absolute distortion of a_r. The positive and negative ε values correspond to contractions and extensions, respectively.

In the absence of structural distortions, i.e. at $\varepsilon = 0$, the crystal field contribution to the density of the magnetic anisotropy energy of the near surface layer would be the same as for an analogous layer in the crystal volume:

$$\sigma_{cfV} = \tfrac{1}{2}N\left[\left(30B^0_{2V} - 450B^0_{4V}\right)\cos^2\vartheta + 525B^0_{4V}\cos^4\vartheta + 15B^{-3}_{4\ V}\cos\vartheta\sin^3\vartheta\sin 3\varphi\right] \quad (11)$$

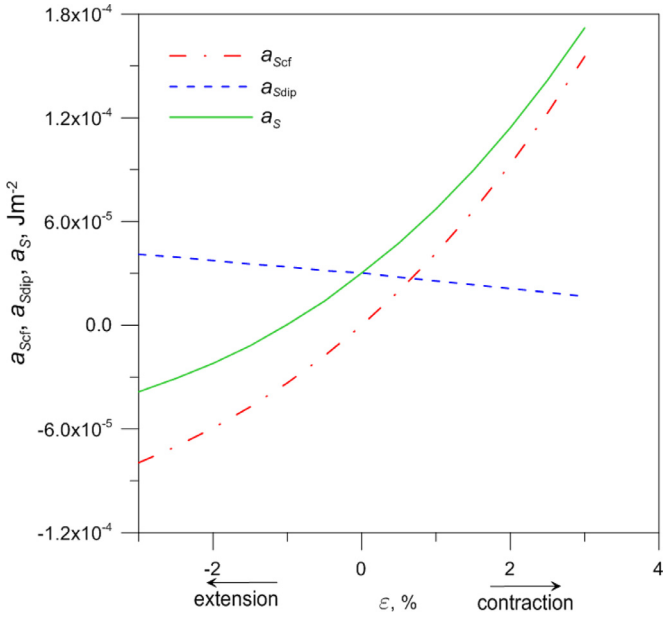

Fig. 4. Values of a_{Scf}, a_{Sdip} [5] and a_S vs. ε at 0 K.

where the *V* subscript refers to the parameter in the volume, and *N* is the same as in Eq. (10).

Thus, σ_{cf}, defined as $\sigma_{cf\,S} - \sigma_{cf\,V}$, can be expressed as:

$$\sigma_{cf} = \sigma_{cf_1}\sin\vartheta\cos\vartheta\sin\varphi + \sigma_{cf_2}\cos^2\vartheta + \sigma_{cf_3}\cos^4\vartheta + \sigma_{cf_4}\sin^2\vartheta\cos^2\varphi + \sigma_{cf_5}\cos\vartheta\sin^3\vartheta\sin 3\varphi \quad (12)$$

where σ_{cf_1}, σ_{cf_2}, σ_{cf_3}, σ_{cf_4} and σ_{cf_5} are defined as the difference between the parameters of matching symmetry terms in Eqs. (10) and (11).

4. Comparison with experimental data

The parameters featuring in Eq. (12) depend on relative distortions and have been calculated for $|\varepsilon| \lesssim 3\%$. The crystal field contribution to the surface magnetic anisotropy energy is a few orders less than the energy required for emergence of the transition layer between the crystal volume and the near surface layer. Thus, the emergence of this layer is still energetically unfavorable, see Introduction, so that $\vartheta = \frac{\pi}{2}$ [4]. So that taking into account Eqs. (10) (12) the crystal field contribution to the surface magnetic anisotropy energy can be expressed as:

$$\sigma_{cf} = -10NB^2_{2S}\sin^2\varphi \quad (13)$$

Comparing Eqs. (13) and (1), we get the crystal field contribution to the surface magnetic anisotropy constant:

$$a_{Scf} = -10NB^2_{2\,S}, \quad (14)$$

and the total surface magnetic anisotropy constant can be expressed as:

$$a_S = a_{Sdip} + a_{Scf}. \quad (15)$$

The $a_{Sdip}(\varepsilon)$ dependence for the layer containing Fe^{3+} ions (D in Fig. 3) has been previously calculated at 300 K [5]. As far as the dipole dipole interaction energy is proportional to the square of magnetization, a_{Sdip} is expected to depend on the temperature as $\mathfrak{M}(T)^2$, $\mathfrak{M}(T)$ being the sublattice magnetization at temperature *T*. Taking into account that $\mathfrak{M}(0\,K)/\mathfrak{M}(300\,K) \approx 1.47$ [15], we have calculated $a_{Sdip}(\varepsilon)$ at 0 K.

Fig. 4 shows the dependences on ε of a_{Sdip} [5], a_{Scf} and a_S at 0 K. Obviously, the distortions much more affect a_{Scf} than a_{Sdip}. According to experimental data [4], in the absence of *H*, in equilibrium $\boldsymbol{l}$ is parallel to C_2; thus, a_S is positive, which corresponds to the case of contractions.

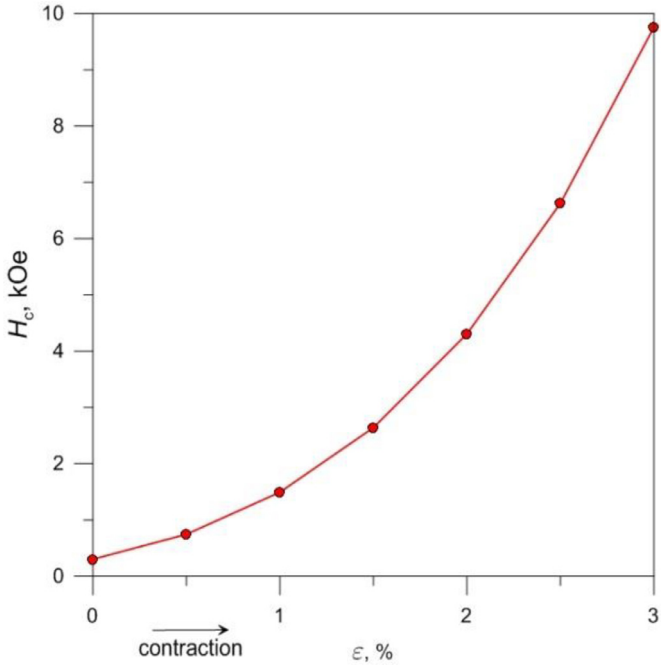

Fig. 5. Calculated $H_c(\varepsilon)$ dependence at 0 K.

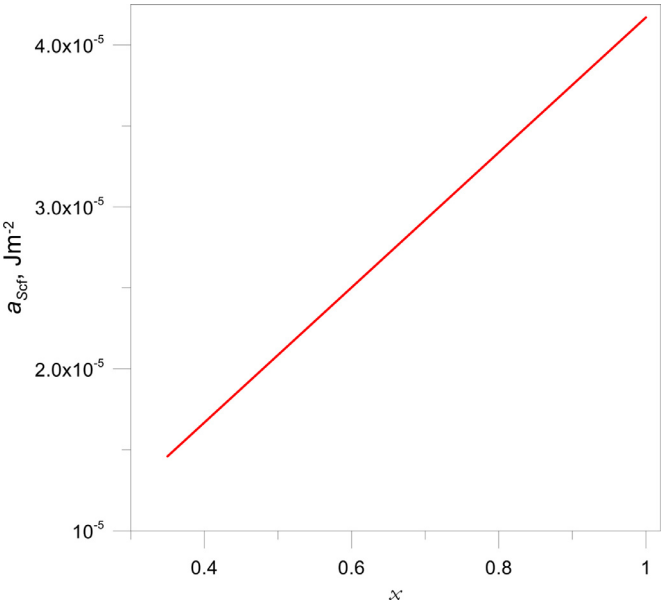

Fig. 6. Calculated dependence of a_{Scf} on x for $\varepsilon = 1\%$ in $Fe_xGa_{1-x}BO_3$ crystals at 0 K.

Indeed, for the near surface layer of ionic crystals contractions rather than extensions are expected [16].

Next, from the $a_S(\varepsilon)$ dependence shown in Fig. 4, we calculate $H_c(\varepsilon)$, see Fig. 5, using the equation similar to Eq. (2):

$$H_c = \frac{4a_S{}^2}{AM} \tag{16}$$

The experimental value of H_c at 300 K, (1 kOe, *vide supra*) and the temperature dependence of H_c, see Fig. 10 in the paper by Zubov et al. [4], suggest that at 0 K $H_c \approx 1.47$ kOe. As one can see from Fig. 5, such H_c value can be attained at a contraction of ca. 1 %.

Note that the crystal surface in itself constitutes a structure defect; nevertheless, other types of structure defects can occur in the near surface layer, for instance, vacancies of magnetic ions. Such defects are also expected to contribute to a_{Scf}. As model objects for studying surface magnetism in crystals with such defects one can consider diamagneti cally diluted iron gallium borates, $Fe_xGa_{1-x}BO_3$, in which case a_{Scf} will depend on x. In Fig. 6 we show the calculated $a_{Scf}(x)$ dependence. Ex perimental studies of surface magnetism in these crystals are in progress in our laboratories.

5. Conclusions

The theory of the surface magnetism of iron borate has been ex tended to include, besides the dipole dipole contribution, the crystal field contribution to the surface magnetic anisotropy energy.

A model of structural distortions in the near surface layer for $(1\,0\,\bar{1}\,4)$ face of iron borate has been developed assuming that ions located in this layer are displaced proportionally to their distance from a reference plane assumed to remain immobile. In order to account for the lowering of symmetry of the ions in the near surface layer, the generalized spin Hamiltonian expressed through tesseral spherical tensor operators has been applied, and the spin Hamiltonian parameters have been calculated using the Newman's superposition model. The crystal field contribution to the density of the surface magnetic anisotropy energy at 0 K has been calculated in perturbation theory. The distortions of iron environment produce a significant crystal field contribution to the surface magnetic anisotropy constant a_S; indeed, the experimental results on the studies of surface magnetism by the magneto optic Kerr effect can be satisfactorily described assuming relative contractions in the near surface layer of ca. 1 %.

Acknowledgments

This work was partially supported by the Russian Foundation for Basic Research and the Ministry of Education, Science and Youth of the Republic of Crimea, in the framework of scientific project grant no. 15 42 01008 "р юг а" and by the V.I. Vernadsky Crimean Federal Univer sity Development Program for 2015 2024 including the participation of one of the authors (K. Seleznyova) in the European School on Magnetism 2017 (Corsica, France).

References

[1] R. Diehl, W. Jantz, B.I. Nolang, W. Wettling, in: E. Kaldis (Ed.), Current Topics in Materials Science, vol. 11, Elsevier, New York, 1984, p. 241.
[2] S. Yagupov, M. Strugatsky, K. Seleznyova, E. Maksimova, I. Nauhatsky, V. Yagupov, E. Milyukova, J. Kliava, Appl. Phys. A 121 (2015) 179.
[3] A.K. Pankratov, M.B. Strugatsky, S.V. Yagupov, Sci. Notes of Taurida National Uni- versity, Ser. Phys. 20 (59) (2007) 64.
[4] V.E. Zubov, G.S. Krinchik, V.N. Seleznyov, M.B. Strugatsky, J. Magn. Magn. Mater. 86 (1990) 105.
[5] E.M. Maksimova, I.A. Nauhatsky, M.B. Strugatsky, V.E. Zubov, J. Magn. Magn. Mater. 322 (2010) 477.
[6] L. Néel, J. Phys. Rad. 15 (1954) 225.
[7] K. Seleznyova, M. Strugatsky, S. Yagupov, N. Postivey, A. Artemenko, J. Kliava, Phys. Status Solidi B 251 (2014) 1393.
[8] D.J. Newman, W. Urban, J. Phys. C 5 (1972) 3101.
[9] D.G. McGavin, W.C. Tennant, J.A. Weil, J. Magn. Reson. 87 (1990) 92.
[10] W.C. Tennant, C.J. Walsby, R.F.C. Claridge, D.G. McGavin, J. Phys.: Condens. Matter 12 (2000) 9481.
[11] J. Kliava, R. Berger, Recent Res. Devel. Non-Crystalline Solids, vol. 3, Transworld Research Network, 2003 ISBN 81-7895-090-1 41.
[12] E. Siegel, K.A. Muller, Phys. Rev. B 19 (1979) 109.
[13] S.A. Al'tshuler, B.M. Kozyrev, EPR in Compounds of Transition Elements, second ed., Wiley & Sons, New York, Toronto, Jerusalem, London, 1974.
[14] L.D. Landau, E.M. Lifshitz, Quantum Mechanics: Non-Relativistic Theory, vol. 3, third ed, Pergamon Press, 1977 ISBN 978-0-08-020940-1.
[15] M. Kadomtseva, R.Z. Levitin, Yu.F. Popov, V.N. Seleznev, V.V. Uskov, Sov. Phys. Solid State 14 (1972) 172.
[16] J.E. Lennard-Jones, B.M. Dent, Proc. R. Soc. London, Ser. A 121 (1928) 247.